Distribution of bedrock and alluvial channels in forested mountain drainage basins

David R. Montgomery*, Tim B. Abbe*, John M. Buffington*, N. Phil Peterson†, Kevin M. Schmidt* & Jonathan D. Stock*

* Department of Geological Sciences, University of Washington, Seattle, Washington 98195-1310, USA
† Simpson Timber Company, Shelton, Washington 98584, USA

Mountain river networks often consist of both bedrock and alluvial channels[1–5], the spatial distribution of which controls several fundamental geomorphological and ecological processes[6,7]. The nature of river channels can influence the rates of river incision and landscape evolution[1,2], as well as the stream habitat characteristics affecting species abundance and aquatic ecosystem structure[8–11]. Studies of the factors controlling the distribution of bedrock and alluvial channels have hitherto been limited to anthropogenic badlands[12]. Here we investigate the distribution of channel types in forested mountain drainage basins, and show that the occurrence of bedrock and alluvial channels can be described by a threshold model relating local sediment transport capacity to sediment supply. In addition, we find that valley-spanning log jams create alluvial channels—hospitable to aquatic life—in what would otherwise be bedrock reaches. The formation of such jams depends critically on the stabilizing presence of logs derived from the largest trees in the riverside forests, suggesting that management strategies that allow harvesting of such trees can have a devastating influence on alluvial habitats in mountain drainage basins.

The spatial distribution of bedrock and alluvial reaches depends on the relation of local transport capacity (q_c) to the bedload sediment supply (q_s) delivered from upstream and across channel banks. A bedrock stream bed indicates a transport capacity in excess of sediment supply ($q_c > q_s$), whereas an alluvial stream bed indicates either a balance or an excess of sediment supply ($q_c \leqslant q_s$) (refs 13,14). A general expression for sediment transport capacity incorporating both drainage area, A, and channel gradient, S, is $q_c = kA^mS^n$, where $m, n > 0$ and k is an empirical variable[15]. In drainage basins with relatively uniform geology, hydrology and vegetation, the sediment supply to a channel reach can be expressed as $q_s = bA^p$, where b and p are empirical variables. Local conditions can cause substantial deviations in either q_c or q_s from basin-wide trends. The critical gradient, S_c, for $q_c = q_s$ may be expressed as

$$S_c = [(b/k)A^{p-m}]^{1/n} \quad (1)$$

in which b, k, p, m and n incorporate local transport capacity, sediment supply characteristics, geology and climate. This critical-slope model therefore predicts that bedrock channels occur where $S > S_c$, and alluvial channels occur where $S \leqslant S_c$. We tested this model against data from field surveys in the Satsop River basin, Washington.

The Satsop River originates in Tertiary basalts in the Olympic mountains, flowing southward over Tertiary marine sandstone and siltstone and Pleistocene till and outwash[16,17] to join the Chehalis River and empty into the Pacific Ocean through Grays Harbor. The study area receives ~2,500 mm of annual rainfall[18] and lies in the *Tsuga heterophylla* vegetation zone[19]. Extensive early twentieth century logging removed the prehistoric forest and industry now harvests naturally regenerated forest. As in most of the Pacific Northwest, early logging practices significantly disturbed stream channels[20], and aggressive programs intended to improve fish habitat removed logs from channels in the 1950s through to the 1980s (ref. 21). Extensive salvage of large cedar logs further diminished the supply of in-channel large woody debris over this same period.

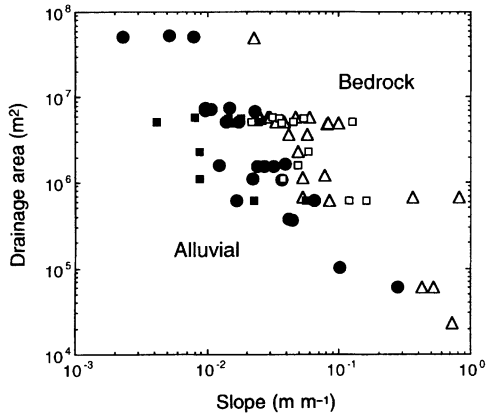

FIG. 1 Plot of drainage area versus reach-average slope for channels in the study area. Larger data points represent channel reaches lacking log jams; open triangles indicate bedrock reaches and solid circles represent alluvial reaches. Smaller data points are from reaches with channel-spanning log jams; solid squares represent forced alluvial reaches immediately upslope of valley-spanning log jams and open squares represent the slope of the underlying bedrock surface, and hence the estimated reach slope in the absence of these jams.

We surveyed continuous topographic profiles down stream-bed centrelines in 59 reaches of the West Fork Satsop River and several tributaries using either a hand-level or tripod-mounted autolevel, rod and tape. We subdivided channels into bedrock or alluvial reaches ranging between 10–20 channel-widths in length, with reach-average slopes and bank full-widths of 0.0023 to 0.81 and 1 to 46 m, respectively. As considered here, bedrock reaches exhibit alluvial cover over lengths of less than a channel width, and alluvial reaches exhibit bedrock exposures of at most a channel width in length. Occasional mixed-morphology reaches with alternating bedrock and alluvial bed surfaces extending downstream for more than a channel width do occur in the study area, but were excluded from this study. We mapped bed morphology and the extent of alluvial terraces and flood plains along two tributaries onto a 1:4,000 scale map of channel thalwegs surveyed using a laser level. We also mapped reach locations onto US Geological Survey 1:24,000 scale topographic maps, from which we determined drainage areas (ranging from 0.02 to 52 km^2) using a digital planimeter.

Slopes of bedrock reaches exceed those of alluvial reaches with comparable drainage areas (Fig. 1). A threshold separating bedrock and alluvial data is well described by an inverse area dependency to the critical slope, predicted by equation (1) for $m > p$. Whereas bedrock channels theoretically plot anywhere above the bedrock/alluvial threshold, non-aggrading alluvial channels would be expected to plot close to the threshold. Thus, scatter within the free-formed alluvial channels may imply that reaches with lower slopes will continue to aggrade until $S = S_c$. Alternatively, such scatter records the magnitude of local variability in sediment supply and transport capacity. Some surveyed reaches showed evidence of recent shallow landsliding from valley walls, and differences in channel confinement may impose local variability to transport capacity. Variance of the alluvial data may also reflect bed armouring and variations in roughness due to large woody debris, which can significantly reduce the transport capacity of forest channels[22]. The threshold shown in Fig. 1, however, indicates that such effects are a secondary influence on the spatial distribution of bedrock and alluvial reaches in the Satsop River basin.

Several processes may transiently affect the distribution of bedrock reaches in mountain drainage basins. Scour by debris flows, for example, can intermittently convert alluvial reaches to a

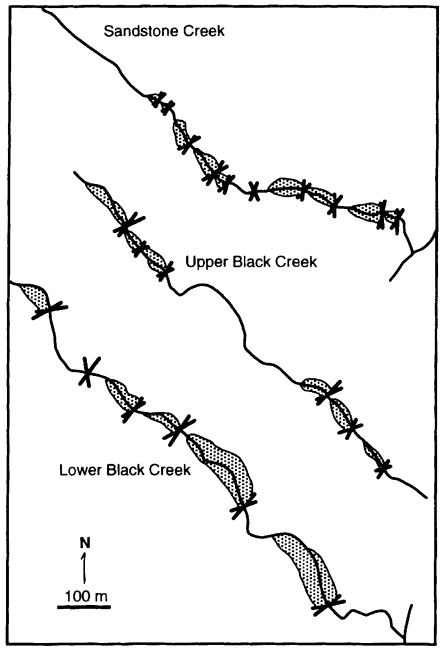

FIG. 2 Maps of southeast-flowing Black and Sandstone creeks showing the distribution of log jams (crosses) and alluvial terraces (stippled).

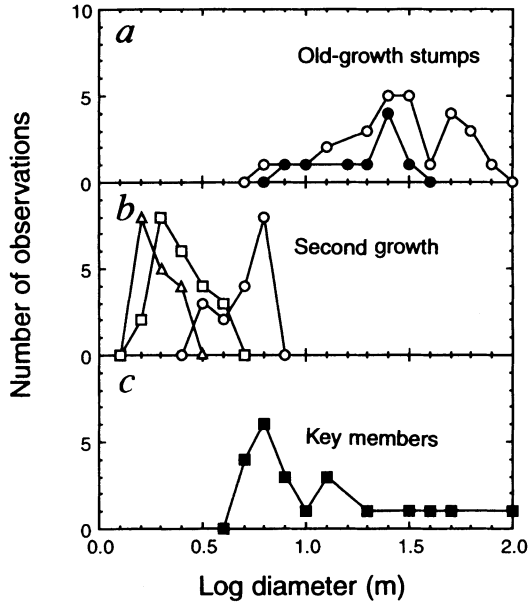

FIG. 3 Frequency distribution of *a*, the diameter of old-growth stumps in the riparian zone; *b*, trees in the current riparian forest; and *c*, key member logs that stabilized valley-spanning log jams. Circles, Douglas fir; filled circles, cedar; squares, hemlock; triangles, alder; filled squares, logs of any species acting to anchor jams (key members).

bedrock morphology. Episodic disturbance such as landslides may introduce and route sediment pulses through mountain channel networks, temporarily converting bedrock reaches to alluvial morphologies[23]. We anticipate that spatial and temporal variations in sediment supply could complicate relations of the kind reported here; local sources of high sediment supply could result in alluvial reaches within the field of bedrock data and locally reduced supply, or increased transport capacity could likewise result in bedrock reaches within the field of alluvial data. Such exceptions to the critical-slope model may prove valuable in interpreting watershed history and conditions, a central focus of watershed analysis efforts in the Pacific Northwest[24].

The introduction of large woody debris can significantly influence channel morphology and aquatic ecosystems in forested environments[25–27]. Individual logs and log jams can dominate pool and bar formation[27–30] and control the local elevation drop in steep forest channels[31,32]. Alluvial terraces and flood plains along surveyed tributaries of the West Fork Satsop River occur as backwater deposits immediately upstream of naturally occurring, valley-spanning log jams (Fig. 2); small terrace remnants lie upslope of both of the breached log jams that lack mappable alluvial deposits. Alluvial deposits, side channels and pools associated with these jams provide aquatic habitat unavailable in bedrock channels.

Longitudinal channel profiles indicate that physical obstruction to sediment movement and backwater effects associated with valley-spanning log jams force deposition of alluvium in otherwise bedrock reaches. In each reach with a valley jam, slopes were determined for the alluvial stream beds immediately upslope of the jam. Bedrock exposed at the base of surveyed jams and in upstream pools allowed determination of the average gradient of the underlying bedrock surface. These data reveal that log jams can force active alluvial beds in otherwise bedrock reaches (Fig. 1) and indicate that jam removal would convert these forced alluvial channels into bedrock reaches. In these mountain channels, the distribution of stable log jams dominates the distribution of alluvial channel reaches.

Individual large logs, in turn, govern the stability of valley-spanning log jams. Field observations demonstrate that the key member logs[27] anchoring the surveyed jams are old-growth remnants and large second-growth trees. Diameters of key members exceed those of all but the largest trees in second-growth riparian forests, but closely correspond to those of prehistoric riparian stumps (Fig. 3). Streamside forest management involving removal of the largest trees and retention of smaller ones[33,34] therefore favours long-term conversion of alluvial reaches to bedrock in those portions of mountain drainage basins where $S > S_c$.

The observation that bedrock channels occur on steeper slopes than alluvial channels of comparable drainage area implies an excess transport capacity that should render bedrock channels relatively insensitive to changes in sediment supply or discharge[35]. Reaches plotting close to the bedrock/alluvial threshold, however, likely represent channels particularly susceptible to land use impact or climate change. Channel networks with short, mixed alluvial and bedrock reaches where $S \approx S_c$ could respond dramatically to even modest changes in sediment supply, discharge or the input of large logs. Our findings support the use of a critical-slope model to discriminate bedrock and alluvial channels in landscape evolution models and suggest the potential for basin-wide predictions of channel type based on limited field surveys. Our results imply that removal of in-stream logs could have devastated much of the upland alluvial habitat in portions of mountain drainage basins in the Pacific Northwest. Furthermore, the large diameter of key member logs currently stabilizing valley-spanning jams implies that persistence of alluvial channel reaches in mountain streams can depend on the presence of old-growth-sized trees. Even the selective harvest of the largest trees in streamside forests may entail profound long-term impacts on aquatic ecosystems in forested mountain drainage basins. □

Received 26 January; accepted 8 May 1996.

1. Seidl, M. A. & Dietrich, W. E.in *Functional Geomorphology: Landform Analysis and Models* (eds Schmidt, K.-H. & de Ploey, J.) 101–124 (Catena suppl. 23, Cremlingen-Destedt, 1992).
2. Howard, A. D., Dietrich, W. E. & Seidl, M. A. *J. geophys. Res.* **99,** 13971–13986 (1994).
3. Brush, L. M. Jr *US Geol. Surv. Prof. Pap. 282-F* (1961).
4. Miller, J. R. *J. Geol.* **99,** 591–605 (1991).
5. Wohl, E. E. *J. Geol.* **101,** 749–761 (1993).
6. Richards, K. *Rivers: Form and Process in Alluvial Channels* (Methuen, New York, 1982).
7. Hynes, H. B. N. *The Ecology of Running Waters* (Univ. Toronto Press, Toronto, 1970).
8. Minshall, G. W. *Hydrobiologia* **32,** 305–339 (1968).
9. Cummins, K. W. & Lauff, G. H. *Hydrobiologia* **34,** 145–181 (1969).
10. Huryn, A. D. & Wallace, A. B. *Ecology* **68,** 1932–1942 (1987).
11. Kondolf, G. M. & Wolman, M. G. *Wat. Resour. Res.* **29,** 2275–2285 (1993).

12. Howard, A. D. & Kerby, G. *Geol. Soc. Am. Bull.* **94,** 739–752 (1983).
13. Gilbert, G. K. *Geology of the Henry Mountains* (US Geog. and Geol. Survey, Govt Print Office, Washington, 1877).
14. Gilbert, G. K. *US Geol. Surv. Prof. Pap. 86* (Govt Print Office, Washington, 1914).
15. Kirkby, M. J. in *Inst. Br. Geogr. Sp. Publ. No. 3* (1971).
16. Logan, R. L. *Geologic Map of the South Half of the Shelton and South Half of the Copalis Beach Quadrangles, Washington* (Open File Report 87–9, Washington Div. Geol. and Earth Resources, 1987).
17. Walsh, T. J., Korosec, M. A., Phillips, W. M., Logan, R. L. & Schasse, H. W. *Geologic Map of Washington—Southwest Quadrant* (Geologic Map GM-34, Washington Div. Geol. and Earth Resources, 1987).
18. Scott, J. W., Vasquez, C. R., Newman, J. G. & Sarjean, B. C. *Washington: A Centennial Atlas* (Center for Pacific Northwest Studies, Western Washington Univ., Bellingham, 1989).
19. Franklin, J. F. & Dyrness, C. T. *Natural Vegetation of Oregon and Washington* (Oregon State Univ. Press, 1988).
20. Sedell, J. R., Leone, F. N. & Duval, W. S. in *Influences of Forest and Rangeland Management on Salmonid Fishes and Their Habitats* (ed. Meehan, W. R.) 325–368 (Am. Fish. Soc., Bethedsa, 1991).
21. Sedell, J. R., Swanson, F. J. & Gregory, S. V. in *Proc. Pacific Northwest Stream Habitat Management Workship* (ed. Hassler, T. J.) 225–245 (Humboldt State University, Arcata, 1984).
22. Buffington, J. M. thesis, Univ. of Washington, Seattle (1995).
23. Benda, L. E. thesis, Univ. of Washington, Seattle (1994).
24. Montgomery, D. R., Grant, G. E. & Sullivan, K. *Wat. Resour. Bull.* **31,** 369–386 (1995).
25. Swanson, F. J. & Lienkaemper, G. W. *USDA Forest Service Gen. Tech. Rep. PNW-69* (1978).
26. Harmon, M. E. *et al. Adv. ecol. Res.* **15,** 133–302 (1986).
27. Abbe, T. B. & Montgomery, D. R. *Reg. Riv.: Res. & Manag.* **12,** 201–221 (1996).
28. Keller, E. A. & Swanson, F. J. *Earth Surf. Proc.* **4,** 361–380 (1979).
29. Lisle, T. E. *Geol. Soc. Am. Bull.* **97,** 999–1011 (1986).
30. Montgomery, D. R., Buffington, J. M., Smith, R., Schmidt, K. M. & Pess, G. *Wat. Resour. Res.* **31,** 1097–1105 (1995).
31. Keller, E. A. & Tally, T. in *Adjustments of the Fluvial System* (eds Rhodes, D. D. & Williams, G. P.) 169–197 (Kendall/Hunt, Dubuque, 1979).
32. Marston, R. A. *Ann. Am. Assoc. Geog.* **72,** 99–108 (1982).
33. Oregon Department of Forestry *Forest Practices Water Protection Rules* ORS Ch. 527.710, OAR Ch. 629-57-2240, 629-57-2260 (1994).
34. Adminsitrative code 222-30-020 (3) (Washington Univ., 1995).
35. Howard, A. D. in *Thresholds in Geomorphology* (eds Coates, D. R. &-Vitek, J. D.) 227–258 (Allen & Unwin, London, 1980).

ACKNOWLEDGEMENTS. We thank Simpson Timber Company and the Washington State Timber/Fish/Wildlife agreement for supporting this research. Discussion with Bill Dietrich and comments by Alan Howard helped clarify our conceptual framework and greatly improved the manuscript.

CORRESPONDENCE should be addressed to D.R.M. (e-mail: dave@bigdirt.geology.washington.edu).

Free-standing and oriented mesoporous silica films grown at the air–water interface

Hong Yang*, Neil Coombs†, Igor Sokolov* & Geoffrey A. Ozin*

* Materials Chemistry Research Group, Lash Miller Chemical Laboratories, University of Toronto, 80 St George Street, Toronto, Ontario, Canada M5S 3H6
† Imagetek Analytical Imaging, 32 Manning Avenue, Toronto, Ontario, Canada M6J 2K4

SURFACTANT assemblies can function as templates for the deposition of silicates to form mesoporous silicas[1]. Recently we described a surfactant-templated synthesis of oriented mesoporous silica films grown at the mica–water interface[2]. Here we show that such films can be grown without a solid substrate, by surfactant templating at the interface between air and water. The films are continuous and have a root-mean-square surface roughness of about 3 Å. They are resilient enough to withstand significant bending, and are sufficiently flexible to be transferred onto substrates of different shapes. We propose a model for film formation which ascribes a dual-templating role to the surfactant: we suggest that both a surfactant overstructure at the air–water interface and micellar aggregates in solution interact collectively with the soluble, polymerizable silicate building blocks. These films might find applications in catalysis, separation technology and biomedicine.

Synthetic methods that enable the fabrication of oriented films of mesostructured materials provide opportunities for detailed studies of their anisotropy and size-tunable properties. This knowledge can be usefully exploited for the development of new technologies that depend on the special properties of this class of materials. Periodic mesostructures that are of current interest include semiconductors[3], metal clusters[4], porous solids[5], composites[6], block-copolymers[7], liquid crystals[8] and patterned self-assembled monolayers[9].

Although oriented mesoporous thin films might find many applications as selective inorganic membranes, those that we described recently grown at the interface between mica and water[2] suffer from several limitations. In particular, few substrates have an atomically smooth surface and can sustain their structural integrity under the corrosive conditions of a synthesis, while at the same time facilitating oriented film formation. We considered that this problem might be surmounted by dispensing with a solid substrate and growing the films instead under surfactant overstructures at the interface between air and water.

The synthesis of mesoporous silica films at the air–water interface under acidic conditions[10] is achieved using the following reactant mole ratios: 100 H_2O : 7 HCl : 0.11 CTACl : 0.07–0.13 TEOS; where CTACl is the cationic surfactant $CH_3(CH_2)_{15}N(CH_3)_3Cl$ and TEOS is the silica source reagent $(C_2H_5O)_4Si$. The surfactant solution is mixed with TEOS and stirred for 2–3 minutes at room temperature and transferred into a polypropylene bottle. The film-forming process works well under static conditions at 80 °C over a reaction time of minutes to days. Well formed films, with thicknesses from tens of nanometres up to about half a micrometre have been grown at the air–liquid interface.

Scanning electron microscopy (SEM) images of the films that have been transferred onto a copper grid reveal that they are continuous, Fig. 1*a*. Polarized optical microscopy images (not shown) recorded at room temperature depict that the films are optically isotropic. This implies that the silica wall material is amorphous and that the micellar assembly contained within the channels is not behaving like a liquid crystal.

Transmission electron microscopy (TEM) images of microtomed sections cut orthogonally to the surface of the as-synthesized free-standing films show that the channels are hexagonally close-packed with a centre-to-centre distance of ~50 Å, Fig. 1*b*. This implies growth of the channels in an orientation parallel to the air–water interface. The observation of a smooth film surface grown at the air–water interface with a root-mean-square roughness of ~3 Å indicates that the growth process occurs via deposition of silica-surfactant micellar solution precursors at a surfactant overstructure localized at this interface. The film surface growing into the solution shows roughness on the mesoscopic scale, which might represent a silica replica of the disposition of micellar structures as they are deposited at this lower surface (Fig. 1*c*).

Early-stage free-standing films, lifted onto TEM grids and viewed directly, are sufficiently thin to be imaged at an accelerating voltage of 50 kV (Fig. 1*d*). Under these conditions, a highly ordered periodic structure with a spacing of ~25 Å is observed. The observed 25 Å periodicity is consistent with a hexagonal close-packed arrangement of one-dimensional channels viewed orthogonally to the film surface[11]. The image is consistent with the proposal that the channels are oriented parallel to the surface of the film. TEM images (not shown) of calcined (450 °C for 4 h in air) free-standing films demonstrate that the mesopore order is intact.

SEM images show that the films are resilient to bending (Fig. 1*e*). They have been transferred onto substrates with different shapes. These properties may reflect the thin organic–inorganic composite nature of the films. Together with complementary powder X-ray diffraction studies, the results demonstrate that the macroscopic integrity and the mesopore order of the attached films are intact.